IEEE Sensors Letters Volume 2(3) (2017)

IEEE Sensors Council

Article Subject (see Index Terms below and write one here)_____

3D Printed Smart Orthotic Insoles: Monitoring a Person's Gait Step by Step

Zhongyang Hao[1], Kevin Cook[2], John Canning[1], Hsiang-Ting Chen[3] and Cicero Martelli[4]

[1]*Interdisciplinary Photonics Laboratories, Tech Lab, School of Electrical & Data Engineering, University of Technology Sydney (UTS), NSW 2007 & 2019 Australia.*

[2]*Faculty of Engineering and Information Technology (FEIT), UTS. University of Technology Sydney (UTS), NSW 2007 & 2019 Australia.*

[3]*Centre of Artificial Intelligence, University of Technology Sydney (UTS), NSW 2007 & 2019, Australia*

[4]*Electrical and Computer Engineering, Federal University of Technology Parana, Curitiba 80230-901, Brazil.*

Abstract—Gait monitoring using a 3D printed smart insole embedded with embedded optical fibre Bragg gratings is reported in this paper. The smart insole combines 3D printing technology and fiber Bragg gratings (FBGs) sensors providing high sensitivity and end-point low cost. Results using pressure points measured by four FBGs are sufficient to differentiate foot loads and gait types.

Index Terms—FBGs 3D printing.

I. INTRODUCTION

Changes in gait are often early indicators of chronic diseases such as stroke, dementia, Parkinson's disease, cancer, cardiac disease and diabetes. The monitoring and detection of gait can also provide sufficient early warning to assist in the prevention and mitigation of injuries in both animals and humans [1-4]. Gait diagnostics is also important more broadly in identifying normal or pathological walking, trotting or running patterns and is used in medical planning, healthcare, rehabilitation, physical therapy, competition preparation and exercise training. For example, with enough detailed gait analysis during rehabilitation training of a patient, animal or human, it is possible to quantify the patient's degree of recovery after surgery and tailor appropriate treatment [5]. Recently, embedded fibre gratings within 3D printed horseshoes demonstrated how photonic fibre sensing technology can significantly benefit gait [6,7]. Extraordinary insight into the nature of blood circulation in a horse was obtained, arising from the compression of the unique vein-filled hooves, creating pressure that has to follow the heartbeat of the animal. A mismatch between this compressive blood release from the four hooves with the heartbeat is, for example, the likely trigger of sudden cardiac arrest of horses in competition. In this work, we extend the use of this technology to human gait analysis, using fibre gratings embedded in 3D printed orthotic insoles placed within a performance shoe.

Commercially available smart insole systems, such as the Pedar insole System [8], offer high-resolution gait monitoring. Unfortunately, they are used only for clinical research, while more inexpensive sensor insoles that might have wider deployment often tend to have poorer resolution and can miss significant information [9]. There are also question marks about current electronic sensing technology and its reliability over time. Yingxiao Wu *et al*. [10] demonstrated a powered electronic sensor system that lasted over 10.5 hours, reflecting some of the upper limits of local power supply. By contrast, optical fibre sensors are established in niche industries, from oil and gas to construction, as long-term alternatives to electronic sensors with less maintenance – the main source of power is signal generation which can be remote through the optical fibre. Many of these are based on passive fibre Bragg gratings (FBGs) which have been used in various industries for a variety of sensor applications, including temperature and strain measurements. By combining these with low cost 3D printing of smart horseshoes or insoles, these parameters can be used to characterize load on an insole at different places, forming the basis for gait analysis used thus far. 3D printing also offers a unique customization that can be better tuned to specific individuals given the varying nature of human feet.

3D printing also offers a unique customization that can be better tuned to specific individuals given the varying nature of human feet. In fact, 3D printing has proven extremely popular for orthotics research allowing customised designs, through laser scanning [11], to be fabricated and tested [12-20]. Despite some concerns about durability and performance they have proven to be extremely effective with the quality of materials and printing improving rapidly. The technique is now commercially available [21, 22].

In this work, we demonstrate the integration of fibre optic sensors and 3D printing to create smart orthotics for human use. Changes in

Corresponding author: John.Canning (John.Canning@uts.edu.au).

plantar pressure lead to shifts in the fibre Bragg grating spectra within the insole and from these shifts the load can be calculated. The sensors are implanted at the main point of the foot: two under the forefoot, and two under the heel [23,24]. Activities such as standing, walking, and going up and down stairs in different postures can be characterized by comparing the different shifts in grating spectra. From this a range of parameters describing the individual's gait can be determined.

II. EXPERIMENTAL DETAILS

The purpose of this exploratory prototype is to verify its feasibility, so this experiment is limited to a single right foot insole, with four points of high-pressure distribution of the foot [25] being monitored.

A. FBG fabrication

FBGs were fabricated in germanium-boron co-doped photosensitive silica fibre (GF1:[GeO_2] ~ 30 mol%; [B_2O_3] ~ 12 mol %). The FBGs are inscribed using direct writing through a phase mask (ArF laser: wavelength λ = 193 nm, pulse fluence f_{pulse} ~ 72 mJ/cm^2, cumulative fluence f_{cum} ~ 86.4 J/cm^2; repetition rate RR = 10 Hz; pulse duration t_w = 15 nm and FBG length L = 10 mm). To reduce cabling complexities whilst allowing the gratings to be lain straight, two gratings are written into each fibre. Fig. 1(a) shows an image of the final insole with grating locations.

B. Design of the smart insole

The size of the insole is designed according to the size of the experimenter's shoes which are a UK size 9. AutoCAD software is used to design the insole. To print the insole, a novel, flexible printing material is utilised: FlexiFil from Formfutura. Appendix 1 summarizes its properties. Printing is undertaken on a low cost Flashforge 3D printer (Dreamer model). Halfway through printing the printing, the optical fibre sensors are added in and then printing is continued. The application of a small weight load, w ~ (5.5 ± 0.1) g, on the fibre ensures constant tension during printing. The final print job introduces compression on the grating, monitored as a decrease in Bragg wavelength, λ_B, [26], ensuring that the gratings are firmly fixed into place. This compression rises from the fact that the solid state of polymers is typically denser than the liquid state. When completed, the insole is post annealed at T = 90 ºC for t ~ 12 hours. After splicing additional cable, the back end of the insole has a protective casing for cabling to be directed upwards (Fig. 1(b)). The next step is to insert the insole into the athletic shoes. The completed prototype is shown in Fig. 1(b).

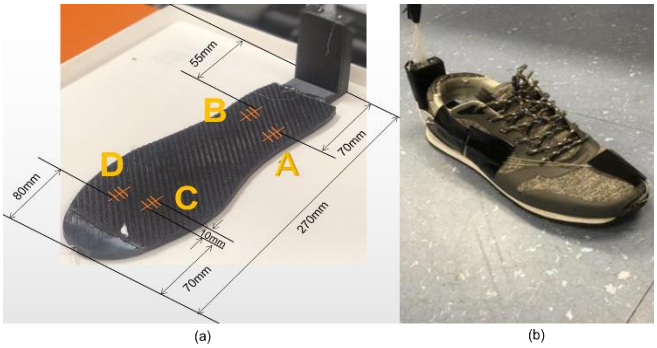

Fig.1. (a) Combined insole, and the four points A, B, C, and D in the figure correspond to four FBG sensors; (b) Prototype

C. Experiment and Data collection

An optical sensing interrogator (a Micron Optics SM130 model) was used to track λ_B of each FBG. The combination of high speed and repeatability allows a single module to dynamically interrogate sensors and measure static sensors with ultra-high resolution. The scan frequency is ν = 1 khz, and the wavelength range is λ = (1510 - 1590) nm. The interrogator records λ_B of the FBGs before and after being implanted in the insole as well as dynamically recording wavelength shifts during various gait modes under test.

Representative actions selected for analysis and recording are:

- Standing still and standing in different ways. Specifically, the center of gravity is placed in the front, rear, left and right directions for repeated standing tests.
- Walking. The most common exercise is walking, an activity that often forms the basis from which to measure other complex movements. By studying the duty cycle of the waveform, the user's walking information can be obtained.

The experiment test subject was the author (Hao) on a flat surface in the room at a constant temperature T = 22.5 ºC, and each set of experiments was limited to one minute.

III. RESULTS

A. Specific parameters of FBGs

Fibre and grating details were provided above. In these experiments we observe that the gratings are substantially chirped. When optimization of the printing process is achieved, grating chirp can be avoided [26]. For this work, however, we can follow the reflection peak and monitor gait. The wavelength, λ_B of the four FBGs before and after embedding into insole are shown in Table 1:

Table 1. Comparison of FBG values before and after embedding within the insole.

Sensor position	T (℃)	Before λ_B(nm) Δ~0.002nm	After λ_B(nm) Δ~0.002nm
A	22.5	1546.131	1538.171
B	22.5	1546.288	1539.155
C	22.4	1543.720	1547.340
D	22.4	1542.194	1532.400

Consistent with material compression as the polymer solidifies after printing, it can be seen from the table that the reflection wavelength of FBGs after implantation shifts to shorter wavelengths by $\Delta\lambda > 10$ nm, a significant load which corresponds to a physical compression of the period $\Delta\Lambda \sim 6$ nm and a total length contraction over the grating of $\Delta L \sim 60$ μm (obtained from $\Delta\lambda/\lambda \sim \Delta\Lambda/\Lambda \sim \Delta L/L$).

Fig. 2(a) and (b) are the spectra of two FBGs on the right side before and after implantation of the insole. As can be seen from the figure, the reflection wavelengths of both FBGs are reduced, which means that they are both compressed during printing. They are also chirped suggesting the compressive pressure distribution is not uniform along the grating length arising principally from the directional load of the weight; that may in part also be due to a non-uniform thickness and/or stress over the insole during printing.

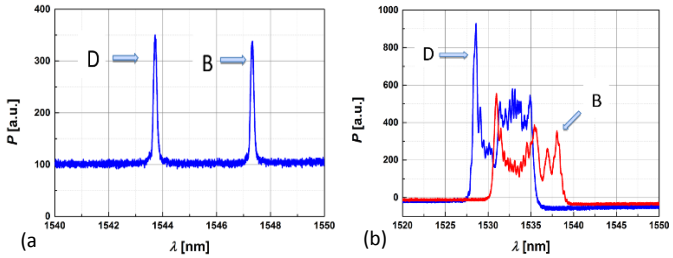

Fig.2. (a) Spectrum of the two FBGs before implementation of insole: (b) Spectrum of two FBGs after embedding within the insole. More than 10 nm shift to shorter wavelengths is observed as well as spectral broadening from non-uniform chirping over $\Delta\lambda \sim 8$ nm for both gratings.

B. Experimental results

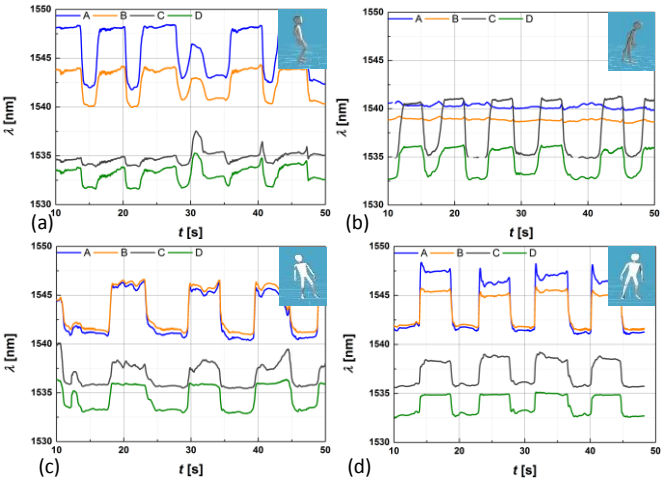

Fig.3. (a) Forward leaning; (b) Backward leaning; (c) Left leaning: (d) Right leaning.

1) Standing:

Fig .3(a) is the result of the forward leaning test. The cycling response reflects repeated lifting of the foot and placing the center of gravity in the front. The four sensors shown in the illustration are the four sensors on the forefoot and the heel. From the plotted data the gray line and the green line (referring to the sensor placed under the forefoot) can be described as cycling square-like waves, and the blue line and the orange line (measurements of the FBGs under the heel) are almost constant. The pressure fluctuations are mainly concentrated on the forefoot. In contrast, the rear heel only slightly fluctuates.

Fig. 3(b) is the result of the backward leaning test. The multiple peaks are the result of repeatedly lifting the foot and placing the center of gravity again. As can be seen from the figure, the blue and orange lines are square waves, while the gray and green lines are almost unchanged, which means that the plantar pressure is mainly distributed in the heel, and the forefoot only has slight fluctuations. Combined with the forward and backward tilt tests, the results reflect the force at the sole of the foot which is consistent with the role that plays in balancing and standing.

Fig. 3(c) and (d) show the test results of left leaning and right leaning standing respectively. It can be seen from the figure that four sensors can reflect the pressure fluctuation of each test. Since the distance between the two sides of the sensor is relatively close, the difference between the left sensor and the right sensor is not obvious.

2) Walking:

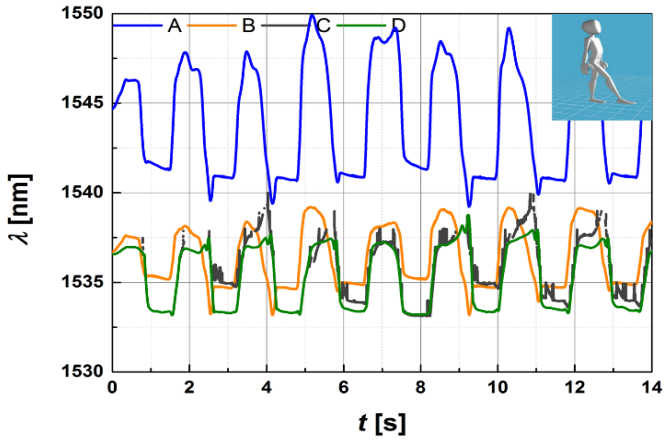

Fig.4 Walking test. Test the FBGs waveform change when walking normally, intercepting the image corresponding to 7 completion steps.

Fig.4 shows the dynamic test for the walk. A total of seven steps of data are recorded in the figure and the image reflects the expected step square response wave. The blue and orange lines are always earlier than the green and gray lines, demonstrating that the system has sufficient response to detect differences in the time of contact with the ground between the front and back parts of the foot. Additional quite important detail is also observed. The heel is the first part of the foot that touches the ground; however, the green and gray lines are the final attenuation because the toes are the last part of the foot off the ground while walking. This reflects the important role toes play in fine tuning balance and enabling smooth walking. By recording the time and the duty cycle of the step, it is possible to analyze the pace and the time between each step and learn the patient's walking habits,

which is in line with expectations. On this basis, combining the technology of embedded FBGs with minimal chirping, we can trace the specified FBGs and find the mapping relationship between various walking postures and FBG wavelength changes.

IV. CONCLUSIONS

A novel route to gait analysis in people has been demonstrated, combining fibre Bragg grating technology with 3D printing. Here, we use flexible, smart insoles within shoes and obtain consistent expected results in a human trial. Future improvements could add additional sensors for thermal analysis, which when coupled to wireless transmitters in more compact future interrogation systems, would be useful for outdoor assessment in the field. For medical and indeed foot assessment the technology now exists to implement this immediately.

Although not explored in detail, the experiment here using only four FBGs has shown to provide significant data and insight into human foot gait, including fine detail in the dynamic analysis that is characteristic of an individual. For example, information about the foots role in walking was easily detected. Some dynamic limitations arising from the limited interrogator bandwidth can be improved using newer interrogator models with higher bandwidths. Nevertheless, the information reported here is already sufficient to determine differences in potential medical conditions, offering a novel diagnostic tool. In terms of relative costs, ongoing research in cheaper and more compact interrogators will increase as the potential of these applications continues to grow.

Fibre optic cables offer very compact and light sensing prototypes that are proved reliable (> 25 years) within telecommunications. They are electromagnetic free and allow many more sensors within the one cable, permitting even more sophisticated analysis with additional sensors that can be added in. These advantages mean that whilst upfront costs are significant at this point in time, fibre optic sensing of gait measurement will grow. The benefits of the data gathered along with their longer-term operation offer significant advantages over current technologies.

V. ACKNOWLEDGEMENTS

Zhongyang acknowledges a UTS Blue Sky scholarship award. All authors gratefully acknowledge the Australian Research Council LIEF Grant (LE100100082).

APPENDIX

Flexifil (produced by Form Furura): Printing temperature: T = (220 – 260) ºC, diameter: ϕ = 1.75 mm, platform temperature: T = 100 ºC, annealing temperature: T = 90 ºC.

REFERENCES

[1] Mustufa Y A, Barton J, O'Flynn B, Davies R, McCullagh P, Zheng H (2015), "Design of a smart insole for ambulatory assessment of gait." In 2015 IEEE 12th International Conference on Wearable and Implantable Body Sensor Networks (BSN) (pp. 1-5). IEEE.

[2] Montero-Odasso M, Hachinski V (2014), "Preludes to brain failure: executive dysfunction and gait disturbances." Neurological Sciences 35.4: 601-604.

[3] Redd C B, Bamberg S J M (2012), "A wireless sensory feedback device for real-time gait feedback and training." IEEE/ASME Transactions on Mechatronics 17.3: 425-433.

[4] Mickle K J, Munro B J, Lord S R, Menz H B, Steele J R (2009). "ISB Clinical Biomechanics Award 2009: toe weakness and deformity increase the risk of falls in older people." Clinical biomechanics, 24(10), 787-791.

[5] Xu W, Huang M C, Amini N, Liu J J, He L, Sarrafzadeh M (2012). "Smart insole: A wearable system for gait analysis." In Proceedings of the 5th International Conference on PErvasive Technologies Related to Assistive Environments (p. 18). ACM..

[6] Martelli C, da Silva J C C, Galvão J R, Schaphauser P E, Dutra G, da Rocha O G, Dreyer U, Di Renzo A B, de Bastos T P, da Silva M T, Pipa D, Janeczko C, Zamarreño C R, Weber G, Loyola M, Martelli, G, Canning J (2018), (INVITED), "Wired Horses", Bragg Gratings, Poling and Photosensitivity (BGPP), OSA Congress, Zurich, Switzerland.

[7] Galvão J R, Di Renzo A B, Schaphauser, P E, Kalinowski A, Canning J, Zamarreño C R, da Silva J C C, Martelli C (2018), "Fiber Bragg Grating Interrogation Techniques Applied to Horse Gait Analysis", IEEE Sensors. 18 (14): 5778-5785.

[8] Putti A B, Arnold G P, Cochrane L, Abboud R J (2007). "The Pedar® in-shoe system: Repeatability and normal pressure values." Gait & posture, 25(3), 401-405.

[9] Tan A M, Fuss F K, Weizman Y, Troynikov O (2015). "Development of a smart insole for medical and sports purposes". Procedia Engineering, 112, 152-156..

[10] Wu Y, Xu W, Liu J J, Huang M C, Luan S, Lee Y (2014). "An energy-efficient adaptive sensing framework for gait monitoring using smart insole." IEEE Sensors Journal, 15(4), 2335-2343.

[11] Telfer S, Woodburn J (2010), The use of 3D surface scanning for the measurement and assessment of the human foot. Foot Ankle Res, 3:19

[12]Wojciechowski E, Chang A, Balassone D, Ford J, Cheng T, Little D, Menezes M, Hogan S, Burns J (2019), "Feasibility of designing, manufacturing and delivering 3D printed ankle-foot orthoses: a systematic review." Journal of Foot and Ankle Research, 12(1).

[13]Creylman V, Muraru L, Pallari J, Vertommen H, Peeraer L. (2013), "Gait assessment during the initial fitting of customized selective laser sintering ankle foot orthoses in subjects with drop foot." Prosthetics Orthot Int., 37:132–8.;

[14]Faustini M C, Neptune R R, Crawford R H, Stanhope S J (2008), "Manufacture of passive dynamic ankle-foot orthoses using selective laser sintering." IEEE Trans Biomed Eng., 55:784–90. 15.

[15]Mavroidis C, Ranky R G, Sivak M L, Patritti B L, DiPisa J, Caddle A, Kara Gilhooly, Govoni L, Sivak S, Lancia M, Drillio R, Bonato P (2011), "Patient specific ankle-foot orthoses using rapid prototyping." Journal of neuroengineering and rehabilitation, 8(1), 1.

[16]Schrank E, Stanhope S (2011), "Dimensional accuracy of ankle-foot orthoses constructed by rapid customization and manufacturing framework." Rehabil Res Dev., 48:31–42.

[17]Schrank E S, Hitch L, Wallace K, Moore R, Stanhope S J (2013), "Assessment of a virtual functional prototyping process for the rapid manufacture of passivedynamic ank le-foot orthoses." Biomech Eng., 135:101011–7. 18.

[18]Telfer S, Pallari J, Munguia J, Dalgarno K, McGeough M, Woodburn J (2012), "Embracing additive manufacture: implications for foot and ankle orthosis design." BMC Musculoskelet Disord.;13:84. 19.

[19]Walbran M, Turner K, McDaid A J (2016), "Customized 3D printed ankle-foot orthosis with adaptable carbon fibre composite spring joint." *Cogent Eng.*, 3: 1227022. 20.

[20]Aydin L, Kucuk S (2018), "A method for more accurate FEA results on a medical device developed by 3D technologies." Polym Adv Technol., 29:2281–6. 21.

[21] Deckers J P, Vermandel M, Geldhof J, Vasiliauskaite E, Forward M, Plasschaert F (2018), "Development and clinical evaluation of laser-sintered ankle foot orthoses." Plast Rubber Compos., 47:42–6

[22]https://www.superfeet.com/en-us/ME3D

[23]https://potterpodiatry.com.au/3d-printed-orthotics/

[24] Zhu H, Wertsch J J, Harris G F, Loftsgaarden J D, Price M B (1991). "Foot pressure distribution during walking and shuffling." Archives of physical medicine and rehabilitation, 72(6), 390-397..

[25] Hessert M J, Vyas M, Leach J, Hu K, Lipsitz L A, Novak V (2005), "Foot pressure distribution during walking in young and old adults." BMC geriatrics 5.1: 8.

[26]Asma Z,Cook K, Canning J(2019), ”Characterisation of FDM filament compression with fibre Bragg Gratings.” 8th Asia Pacific Opt. Sensors Conf. (APOS 2019), Auckland, New Zealand.